J. of Supercritical Fluids 48 (2009) 99–107

Contents lists available at ScienceDirect

The Journal of Supercritical Fluids

journal homepage: www.elsevier.com/locate/supflu

High pressure phase behavior of carbon dioxide in 1-alkyl-3-methylimidazolium bis(trifluoromethylsulfonyl)imide ionic liquids

Pedro J. Carvalho[a], Víctor H. Álvarez[c], José J.B. Machado[a], Jérôme Pauly[b], Jean-Luc Daridon[b], Isabel M. Marrucho[a], Martín Aznar[c], João A.P. Coutinho[a,*]

[a] CICECO, Departamento de Química, Universidade de Aveiro, 3810-193 Aveiro, Portugal
[b] Laboratoire des Fluides Complexes, UMR 5150, BP 1155, 64013 Pau Cedex, France
[c] Faculdade de Engenharia Química, Universidade Estadual de Campinas, 13083-970 Campinas-SP, Brazil

ARTICLE INFO

Article history:
Received 8 August 2008
Received in revised form 9 October 2008
Accepted 10 October 2008

Keywords:
1-Ethyl-3-methyl-imidazolium bis(trifluoromethylsulfonyl)imide
1-Methyl-3-pentyl-imidazolium bis(trifluoromethylsulfonyl)imide
Carbon dioxide
Phase behavior
Supercritical
Experimental
High pressure

ABSTRACT

New standards concerning environmental and safety issues are creating an increasing interest on ionic liquids as alternative solvents for a wide range of industrial applications. In this work, a new apparatus developed to measure vapor–liquid phase equilibrium in a wide range of pressures and temperatures was used to measure the phase behavior of the binary systems of carbon dioxide (CO_2) + 1-ethyl-3-methyl-imidazolium bis(trifluoromethylsulfonyl)imide ([C_2mim][Tf_2N]) and CO_2 + 1-methyl-3-pentyl-imidazolium bis(trifluoromethylsulfonyl)imide ([C_5mim][Tf_2N]) at temperatures up to 363 K and pressures up to 50 MPa. A thermodynamic consistency test, developed for systems with incomplete *PTxy* data and based on the Gibbs–Duhem equation, was applied to the experimental data measured in this work and the Peng–Robinson EoS using the Wong–Sandler mixing rule was used to describe the experimental data with excellent results.

1. Introduction

Ionic liquids (ILs), a class of *neoteric* solvents composed of large organic cations and organic or inorganic anions, that cannot form an ordered crystal and thus remain liquid at or near room temperature, are becoming one of the fastest growing "green" media for chemists and engineers, bridging academia and industrial interests. The tunable properties of ILs through an endless combination of cations and anions, allow the design of solvents for the development of more efficient processes and products. Among the several applications foreseeable for ionic liquids such as solvents in organic synthesis [1,2], homogeneous and biphasic transfer catalysts [3–5], separation processes [6–9], their use in processes with supercritical gases is one of the most exciting.

Blanchard et al. [9–11] described several potential applications of supercritical fluids with ILs. They demonstrated the possibility of using supercritical CO_2 to remove a solute from an IL, without contamination of the extracted solute, solving one of the shortcomings of the use of ionic liquids in solvent extraction processes: the recovery of the compounds from the ionic liquid media. Scurto et al. [12] proposed an innovative process of separating ILs from organic solvents using supercritical CO_2 that induces a phase separation, due to the organic liquid phase expansion and the dielectric constant decrease, forcing the IL to separate into a second liquid phase. Later, Scurto et al. [13] also demonstrated that separation of aqueous solutions of both hydrophobic and hydrophilic ILs can be performed using supercritical CO_2.

A large amount of work concerning the development of ionic liquids with special affinity towards CO_2 has been carried Bates et al. [6] who reported amine functionalized ILs, while Yuan et al. [14] and Sun et al. [15] used hydroxyl-functionalized ILs as a novel efficient catalyst for chemical fixation of CO_2. Yu et al. [16] and Huang et al. [17] proposed guanidinium-based ILs, where the electron-donating groups increased the strength of the donor-acceptor interactions on $-NH_2$ and consequently enhanced the interactions between $-NH_2$ and CO_2. Muldoon et al. [18] and Lopez-Castillo [19] reported that CO_2 can be used to enhance the solubility of other gases that typically present low solubilities in ILs. Solinas et al. [20] showed that inducing CO_2 pressure on a system improves the activation, tuning and immobilization of chiral iridium catalysts in IL/CO_2 for the enantioselective hydrogenation reaction of imines.

* Corresponding author. Tel.: +351 234 401 507; fax: +351 234 370 084.
E-mail address: jcoutinho@ua.pt (J.A.P. Coutinho).

0896-8446/$ – see front matter © 2008 Elsevier B.V. All rights reserved.
doi:10.1016/j.supflu.2008.10.012

The successful development of IL-based processes using supercritical fluids depends on the adequate knowledge of the phase behavior of the systems. Several authors, such as Brennecke [11,21,22], Peters [23–25] Noble [26], Lim [27], Baltus [28], Outcalt [29], Yokozeki [30] and Majer [31], have been reporting supercritical carbon dioxide solubility in common ILs, but few have focused their studies on the Tf_2N anion-based ionic liquids [23,25–29].

Apart task specific ILs, the Tf_2N anion-based ILs are the ones presenting the highest CO_2 solubility. Although both anion and cation influence the CO_2 solubility, the anion has the strongest influence [21,22,32,33]. The presence of fluoroalkyl groups, known to be "*CO_2-philic*", make the Tf_2N anion-based ILs compounds with great CO_2 solubilities. However, this behavior is yet poorly understood and while some authors emphasize the role of the interactions between the CO_2 and the Tf_2N anion [21,22,34], others identify the large free volume of the ionic liquid as the main factor responsible for the large solubility [18]. On the other hand, the alkyl chain length of the cations, also influences the CO_2 solubility, indicating an entropic, rather than enthalpic, effect is present [21]. For a given cation, the data available seems to indicate that the longer the alkyl chain, the higher the free volume, and consequently the larger the solubility [11,21,23,24,34–37].

In this work, a new apparatus was developed to investigate the high pressure phase behavior of gas + ionic liquid systems. Two Tf_2N-based ionic liquids were selected in order to further contribute for a more detailed knowledge and thus a better understanding of the solubility of supercritical CO_2 in these fluids. The system of CO_2 + 1-ethyl-3-methyl-imidazolium bis(trifluoromethylsulfonyl)imide ($[C_2mim][Tf_2N]$) was chosen because it allows the evaluation of the quality of the measurements by direct comparison with literature data [25], and the CO_2 + 1-methyl-3-pentyl-imidazolium bis(trifluoromethylsulfonyl)imide ($[C_5mim][Tf_2N]$) system was studied to investigate the effect of the alkyl chain length on the CO_2 solubility in ionic liquids. Both systems were measured at temperatures up to 363 K and pressures of 50 MPa.

A thermodynamic consistency test [38,39], developed for systems with incomplete *PTxy* data and based on the Gibbs–Duhem equation, and the Peng–Robinson equation of state [40] with the Wong–Sandler mixing rule [41] using the UNIQUAC model [42] for the activity coefficients, was applied to describe the experimental data measured in this work. It will be shown that the model provides an excellent representation of the experimental data and the consistency test shows that the data here reported, unlike many other systems available in the literature, is thermodynamically consistent [38,39,43].

2. Experimental

2.1. Materials

Two imidazolium-based ILs, 1-ethyl-3-methyl-imidazolium bis(trifluoromethylsulfonyl)imide, $[C_2mim][Tf_2N]$ and 3-methyl-1-pentyl-imidazolium bis(trifluoromethylsulfonyl)imide, $[C_5mim][Tf_2N]$, were used on this study. All compounds were acquired from IoLiTec with mass fraction purities >99% and bromide impurity mass fraction $<10^{-4}$. The purities of each ionic liquid stated by the supplier, were checked by ^1H NMR, ^{13}C NMR and ^{19}F NMR.

It is well established that ILs physical properties are influenced by their water content [44–47]. To reduce to negligible values both water and volatile compounds content, vacuum (0.1 Pa), stirring and moderate temperature (353 K), for a period of at least 48 h, were applied prior to the measurements. The final IL water content was determined with a Metrohm 831 Karl Fischer coulometer, indicating a water mass fraction of $(42 \text{ and } 20) \times 10^{-6}$ for $[C_2mim][Tf_2N]$ and $[C_5mim][Tf_2N]$, respectively.

The CO_2 used was from Air Liquide with a purity of ≥99.998% and H_2O, O_2, C_nH_m, N_2 and H_2 impurities volume fractions lower than $(3, 2, 2, 8 \text{ and } 0.5) \times 10^{-6}$, respectively.

2.2. Experimental measurements

The high pressure equilibrium cell developed in this work uses the synthetic method and is sketched in Fig. 1. The cell, based on the design of Daridon and co-workers [48–52], consists of a horizontal hollow stainless-steel cylinder, closed at one end by a movable piston and at the other end by a sapphire window. This window, along with a second window on the cell wall through which an optical fiber lights the cell chamber, allows the operator to follow

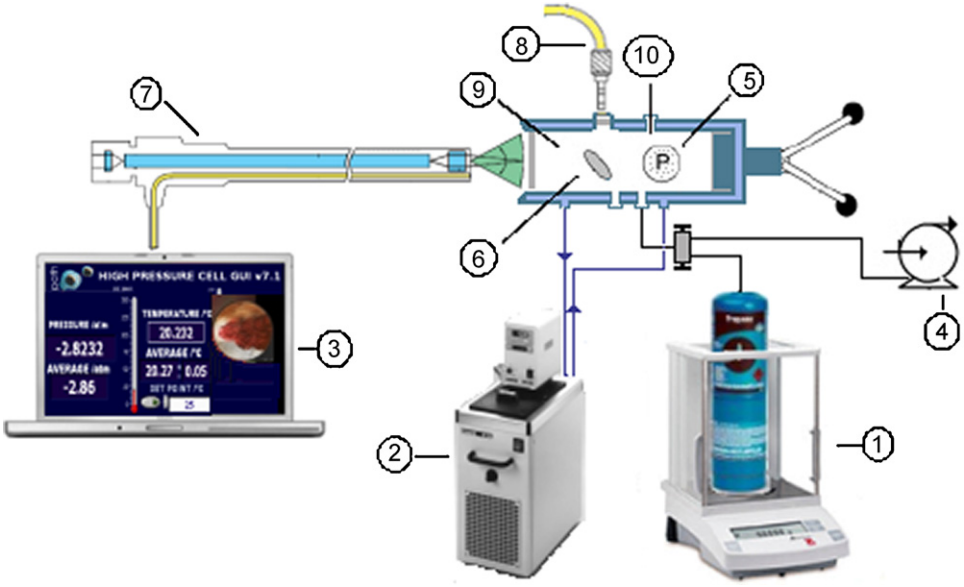

Fig. 1. Schematic apparatus—1: analytical balance; 2: thermostatized bath circulator; 3: computer to data and video acquisition; 4: vacuum pump; 5: piezoresistive pressure transducer; 6: magnetic bar; 7: endoscope plus a video camera; 8: light source with optical fiber cable; 9: high-pressure variable-volume cell; 10: temperature probe.

the behavior of the sample with pressure and temperature. The orthogonal positioning of both sapphire windows minimizes the parasitic reflections and improves the observation in comparison to axial lighting.

A small magnetic bar placed inside the cell allows the homogenization of the mixture by means of an external magnetic stirrer. The sapphire window on the cell wall limits the minimum internal volume of the cell to 8 cm^3, while the maximum value is set to 30 cm^3. The presence of the magnetic stirrer, as well as the cell reduced volume, help to minimize the inertia and temperature gradients within the sample.

The cell is thermostatized by circulating a heat-carrier fluid through three flow lines directly managed into the cell. The heat-carrier fluid is thermo-regulated with a temperature stability of ±0.01 K by means of a thermostat bath circulator (Julabo MC). The temperature is measured with a high precision thermometer, Model PN 5207 with an accuracy of 0.01 K, connected to a calibrated platinum resistance inserted inside the cell close to the sample. The pressure is measured by a piezoresistive silicon pressure transducer (Kulite) fixed directly inside the cell to reduce dead volumes, that was previously calibrated and certified by an independent laboratory with IPAC accreditation, following the EN 837-1 standard and with accuracy better than 0.2%.

A fixed amount of IL was introduced inside the cell, its exact mass was determined by weighting, using a high weight/high precision balance with an accuracy of 1 mg (Sartorius). In order to avoid any interference of atmospheric gases during the manipulation, after placing the IL inside the cell, it was kept under vacuum overnight, while stirring and heating at 353 K.

The CO_2 was introduced under pressure from an aluminum reservoir tank. Its mass was measured with the precision balance and introduced into the measuring cell by means of a flexible high pressure capillary.

After preparation of a mixture of known composition and the desired temperature at low pressure was reached, the pressure was then slowly increased at constant temperature until the system becomes monophasic. The pressure at which the last bubble disappears represents the equilibrium pressure for the fixed temperature.

The purity of the IL is re-checked by NMR at the end of the study to confirm that no degradation of the IL takes place during the measurements.

3. Thermodynamic modeling and consistency

Valderrama and Álvarez [39] developed a thermodynamic consistency test for systems with incomplete *PTxy* data, cataloging them as thermodynamic consistent (TC), thermodynamic inconsistent (TI) or not full consistent (NFC). The authors analyzed the difficulties normally found when modeling this type of mixtures and proposed a methodology to analyze the experimental data, concluding about their thermodynamic consistency or inconsistency. Recently, Álvarez and Aznar [38,43] applied an extension of this approach to several supercritical fluid + IL systems using a method based on the Gibbs–Duhem equation, on the fundamental phase equilibrium equation, and on the Peng–Robinson equation of state [40], with the Wong–Sandler mixing rule [41] using the UNIQUAC model [42] for the activity coefficient.

The test uses the Gibbs–Duhem equation expressed in the integral form, where the left-hand side is denoted as A_P and the right-hand side as A_ϕ, as it follows:

$$A_P = \int \frac{1}{Py_2} dP \tag{1}$$

$$A_\varphi = \int \frac{(1-y_2)}{y_2(Z-1)} \frac{d\varphi_1}{\varphi_1} + \int \frac{1}{Z-1} \frac{d\varphi_2}{\varphi_2} \tag{2}$$

The values for A_P are obtained with experimental Py_2 data, and the values for A_ϕ are obtained with calculated values of Z, ϕ_i and y_2. The subscripts 1 and 2 denote CO_2 and ionic liquid compounds, respectively. The individual percent area deviation, ΔA_i, is given as:

$$\Delta A_i = 100 \left[\frac{A_\varphi - A_P}{A_P} \right]_i \tag{3}$$

where the subscript i refers to the ith data point. The quality of the correlation was analyzed through the relative deviations in the calculated pressure and solute concentration in the gas phase for each point i, defined as:

$$\Delta P_i = 100 \left(\frac{P_i^{cal} - P_i^{exp}}{P_i^{exp}} \right) \tag{4}$$

$$\Delta y_{2_i} = 100 \left[\frac{y_2^{cal} - y_2^{exp}}{y_2^{exp}} \right]_i \tag{5}$$

The method implies the minimization of the deviations of Eqs. (3)–(5), setting as the objective function, OF, for the consistency test the minimization of the deviations in VLE data and the individual percent area deviation.

$$\mathrm{OF} = \sum_{i=1}^{N-1} \left[\frac{A_P - A_\varphi}{\sigma_A} \right]_i^2 + \sum_{i=1}^{N} \left[\frac{P^{cal} - P^{exp}}{\sigma_P} \right]_i^2 + \sum_{i=1}^{N} \left[\frac{y_{fluid}^{cal} - 1}{\sigma_y} \right]_i^2 \tag{6}$$

where N is the number of data points, P is the pressure, y_{fluid} is the vapor mole fraction of the supercritical fluid for data point i, the superscripts "exp" and "cal" refers to the experimental and calculated values, respectively, and σ_A, σ_P and σ_y are the standard deviations of those quantities. The experimental uncertainties in the pressure data were used for σ_P, the value 10^{-5} for σ_y and the value of A_P for σ_A. The minimization method was performed using a genetic algorithm code, implemented and fully explained in Álvarez et al. [53]. The difference between experimental and calculated values was calculated as the average percent deviation, expressed in absolute form, as follows:

$$\left| \Delta P \right| = \frac{100}{N} \sum_{i=1}^{N} \left[\frac{\left| P_i^{cal} - P_i^{exp} \right|}{P_i^{exp}} \right] \tag{7}$$

The isopleths were interpolated with the method proposed by Álvarez and Aznar [43] and the results are shown in Table 1, for the CO_2 + [C_2mim][TF_2N] system and for the CO_2 + [C_5mim][TF_2N] system, respectively. The physical properties used in the model for all substances are reported in Table 2.

4. Results and discussion

Although measurements were previously carried by us and others in similar apparatuses [48–52], [C_2mim][Tf_2N] was selected to validate the methodology and experimental procedure adopted in this work and the measurements were compared against data by Schilderman et al. [25]. High pressure binary vapor–liquid mixtures data of CO_2 in ILs are scarce and significant discrepancies among data from different authors [25,27,29] are common in literature. The identification of the data with the highest quality available in the literature was carried using the thermodynamic consistency test described above [43]. The most reliable data identified by Àlvarez and Aznar [38,43] were those by Schilderman et al. [25] for the system CO_2 + [C_2mim][Tf_2N], where the isotherms at 313 K, 323 K and

Table 1
Interpolated VLE data for the system supercritical CO_2 (1) + [C_2mim][Tf_2N] (2) and CO_2 (1) + [C_5mim][Tf_2N] (2).

	x_1								
T/K	0.221	0.327	0.418	0.503	0.56	0.606	0.65	0.7	0.75
CO_2 (1) + [C_2mim][Tf_2N] (2)									
293.15	–	–	–	–	2.935	3.437	3.942	4.783	
298.15	0.718	1.284	1.915	2.699	3.342	3.922	4.540	5.520	19.065
303.15	0.830	1.453	2.178	3.049	3.784	4.459	5.178	6.497	22.207
313.15	1.073	1.861	2.746	3.835	4.772	5.687	6.681	10.142	28.178
323.15	1.341	2.293	3.372	4.724	5.899	7.121	8.561	14.477	33.729
333.15	1.634	2.757	4.054	5.706	7.164	8.762	10.902	18.933	38.862
343.15	1.953	3.280	4.792	6.770	8.568	10.608	13.585	23.085	43.575
353.15	2.297	3.849	5.587	7.907	10.110	12.660	16.464	27.039	–
363.15	2.666	4.406	6.439	9.105	11.791	14.919	19.429	30.832	–
	x_1								
T/K	0.212	0.351	0.39	0.453	0.619	0.654	0.701	0.751	0.802
CO_2 (1) + [C_5mim][Tf_2N] (2)									
298.15	0.702	1.483	1.718	2.143	3.872	4.429	5.205	8.065	29.980
303.15	0.807	1.664	1.905	2.393	4.352	5.005	5.937	10.577	32.753
313.15	1.028	2.050	2.341	2.938	5.445	6.343	7.723	15.399	38.148
323.15	1.266	2.465	2.817	3.540	6.701	7.919	10.281	19.950	43.205
333.15	1.520	2.912	3.345	4.195	8.103	9.717	13.185	24.231	47.993
343.15	1.792	3.388	3.895	4.899	9.635	11.724	16.461	28.241	52.435
353.15	2.080	3.895	4.447	5.647	11.280	13.925	19.720	31.981	56.153

363 K were found to be thermodynamically consistent. A comparison between our data and the data reported by Schilderman et al. [25] showed a good agreement. Moreover, as will be shown below, the data here measured was found to be essentially thermodynamic consistent.

The solubility of carbon dioxide in the studied ILs was measured for mole fractions from (0.2 to 0.8), in the temperature range (293–363) K and pressures from (0.6 to 50) MPa, as reported in Tables 3 and 4 and depicted in Fig. 2a and b. The temperature increase leads to an increase on the equilibrium pressure and by increasing CO_2 concentration, the equilibrium pressures increase gradually, at first, and rapidly for higher CO_2 contents.

Due to the presence of fluoroalkyl groups, Tf_2N anion-based ILs, are "*CO_2-philic*", meaning that they present higher CO_2 solubilities than other ILs resulting in lower equilibrium pressures for high CO_2 mole fractions, as can be seen in Fig. 2. This behavior, yet poorly understood, seems to be related to the interaction between the negative fluorine atoms and the positive charge on the carbon of the CO_2 molecule [21,22].

It is known that the substituents on the imidazolium ring can affect the ILs properties [23,24,44,47,54–57]. For CO_2, a slight increase on solubility can be observed with the alkyl chain length at all pressures as shown in Fig. 3 [11,21,23,25]. Nonetheless, in the Tf_2N-based ILs, the alkyl chain length on the imidazolium ring seem to have a lower influence on the solubility than other IL families, even for higher CO_2 concentrations [21,25]. Kazarian et al. [58], using ATR–IR spectroscopy, suggested that the increase in solubility is not related to any specific interactions between the CO_2 and the cation. Shariati et al. [23] and Aki et al. [21]

Table 2
Properties of the substances used in the modeling.

Compound	T_c/K	p_c/MPa	ω	r	q
CO_2	304.21[a]	7.38[a]	0.2236[a]	3.26[c]	2.38[c]
[C_2mim][Tf_2N]	1214.22[b]	3.37[b]	0.2818[b]	28.77[c]	18.16[c]
[C_5mim][Tf_2N]	1249.43[b]	2.63[b]	0.4123[b]	34.23[c]	21.84[c]

[a] [61].
[b] [62].
[c] [38].

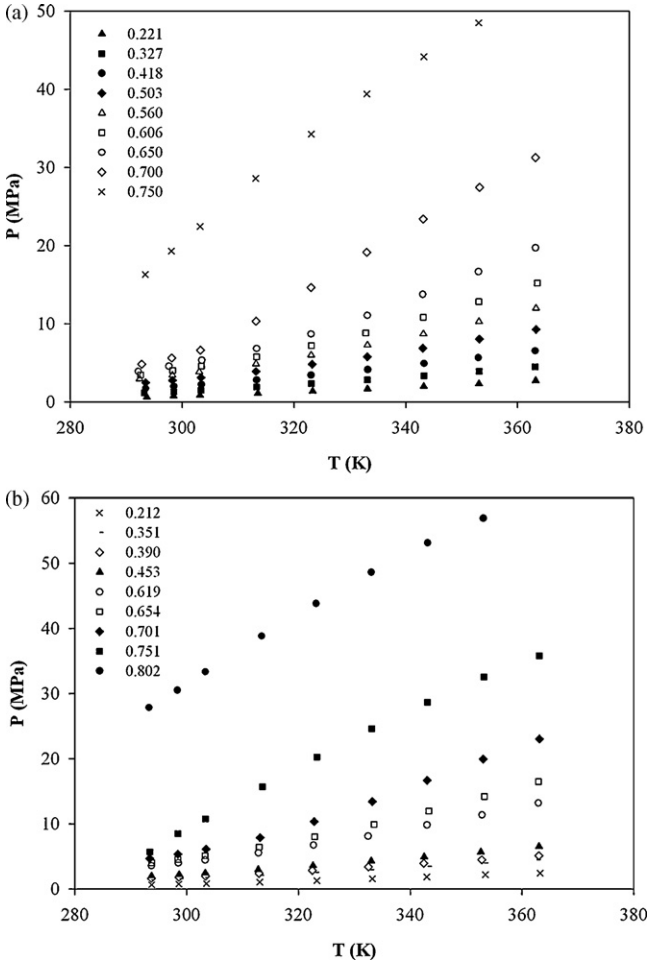

Fig. 2. Pressure–temperature diagram of the binary systems (a) CO_2 + [C_5mim][Tf_2N] and (b) CO_2 + [C_2mim][Tf_2N].

Table 3
Bubble point data for the system CO_2 (1) + [C_2mim][Tf_2N] (2).

x_1	T/K	p/MPa	x_1	T/K	p/MPa	x_1	T/K	p/MPa	x_1	T/K	p/MPa	x_1	T/K	p/MPa
0.221	293.65	0.620	0.327	293.24	1.130	0.418	293.50	1.688	0.503	293.50	2.398	0.560	292.41	2.879
0.221	298.52	0.725	0.327	298.50	1.295	0.418	298.55	1.945	0.503	298.29	2.706	0.560	298.24	3.351
0.221	303.25	0.837	0.327	303.41	1.462	0.418	303.48	2.185	0.503	303.41	3.076	0.560	303.11	3.778
0.221	313.59	1.083	0.327	313.32	1.868	0.418	313.32	2.745	0.503	313.24	3.845	0.560	313.22	4.780
0.221	323.39	1.345	0.327	323.13	2.292	0.418	323.10	3.365	0.503	323.27	4.725	0.560	323.07	5.883
0.221	333.15	1.645	0.327	333.17	2.758	0.418	333.23	4.054	0.503	333.16	5.708	0.560	333.16	7.173
0.221	343.25	1.957	0.327	343.27	3.287	0.418	343.30	4.836	0.503	343.11	6.769	0.560	343.19	8.569
0.221	353.10	2.276	0.327	353.16	3.850	0.418	353.02	5.565	0.503	353.18	7.912	0.560	353.14	10.115
0.221	363.23	2.680	0.327	363.19	4.408	0.418	363.17	6.436	0.503	363.35	9.128	0.560	363.34	11.821

x_1	T/K	p/MPa	x_1	T/K	p/MPa	x_1	T/K	p/MPa	x_1	T/K	p/MPa
0.606	292.60	3.387	0.650	292.16	3.825	0.700	292.82	4.736	0.750	293.44	16.076
0.606	298.29	3.942	0.650	297.70	4.485	0.700	298.15	5.520	0.750	298.09	19.048
0.606	303.46	4.506	0.650	303.54	5.230	0.700	303.30	6.535	0.750	303.26	22.130
0.606	313.30	5.686	0.650	313.35	6.715	0.700	313.24	10.180	0.750	313.19	28.187
0.606	323.11	7.103	0.650	323.10	8.550	0.700	323.09	14.450	0.750	323.14	33.787
0.606	332.88	8.695	0.650	333.16	10.905	0.700	333.04	18.885	0.750	333.08	38.898
0.606	343.13	10.649	0.650	343.08	13.565	0.700	343.15	23.085	0.750	343.29	43.565
0.606	353.07	12.650	0.650	353.05	16.435	0.700	353.22	27.066	0.750	353.08	47.850
0.606	363.55	14.996	0.650	363.22	19.450	0.700	363.22	30.858			

Table 4
Bubble point data the system CO_2 (1) + [C_5mim][Tf_2N] (2).

x_1	T/K	p/MPa	x_1	T/K	p/MPa	x_1	T/K	p/MPa	x_1	T/K	p/MPa	x_1	T/K	p/MPa
0.212	298.65	0.720	0.351	298.77	1.517	0.390	298.65	1.736	0.453	298.70	2.152	0.619	298.55	3.915
0.212	303.61	0.799	0.351	303.34	1.675	0.390	303.39	1.915	0.453	303.38	2.395	0.619	303.33	4.360
0.212	313.15	1.044	0.351	313.21	2.031	0.390	312.99	2.334	0.453	312.85	2.927	0.619	312.90	5.426
0.212	323.35	1.252	0.351	323.05	2.468	0.390	322.52	2.785	0.453	322.62	3.512	0.619	322.72	6.645
0.212	333.25	1.525	0.351	332.85	2.894	0.390	332.54	3.312	0.453	333.07	4.218	0.619	332.50	7.984
0.212	343.00	1.780	0.351	343.19	3.398	0.390	342.47	3.858	0.453	342.53	4.839	0.619	343.04	9.650
0.212	353.49	2.124	0.351	353.26	3.907	0.390	352.85	4.430	0.453	352.65	5.598	0.619	352.86	11.212
0.212	363.29	2.370	0.351	362.68	4.400	0.390	363.05	5.050	0.453	363.05	6.430	0.619	362.95	12.990
0.212	293.75	0.618	0.351	293.65	1.322	0.390	293.73	1.564	0.453	293.75	1.943	0.619	293.75	3.486

x_1	T/K	p/MPa	x_1	T/K	p/MPa	x_1	T/K	p/MPa	x_1	T/K	p/MPa
0.654	298.47	4.460	0.701	298.45	5.245	0.751	298.42	8.365	0.802	298.37	30.098
0.654	303.32	5.030	0.701	303.49	5.990	0.751	303.38	10.625	0.802	303.38	32.881
0.654	313.00	6.344	0.701	313.19	7.732	0.751	313.57	15.435	0.802	293.30	27.460
0.654	322.96	7.870	0.701	322.85	10.198	0.751	323.34	19.995	0.802	313.44	38.299
0.654	333.56	9.778	0.701	333.28	13.225	0.751	333.11	24.280	0.802	323.19	43.225
0.654	343.37	11.776	0.701	343.08	16.438	0.751	343.05	28.266	0.802	333.08	47.960
0.654	353.30	13.980	0.701	353.06	19.692	0.751	353.20	32.086	0.802	343.14	52.431
0.654	362.95	16.246	0.701	363.12	22.730	0.751	363.11	35.340	0.802	353.13	56.146
0.654	293.76	3.974	0.701	293.43	4.617	0.751	293.42	5.609	0.802	363.29	59.805

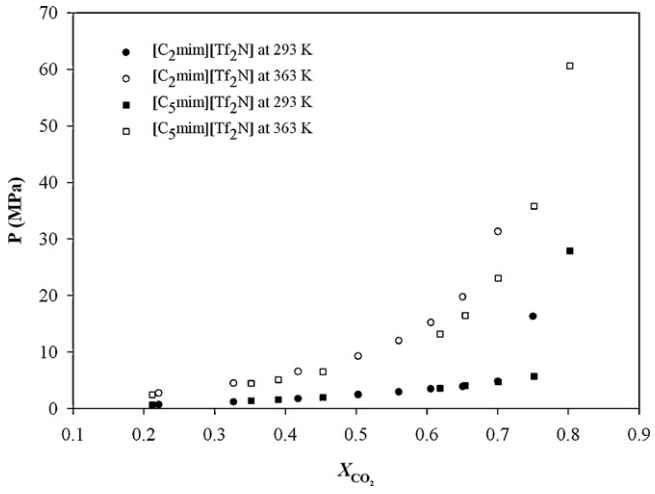

Fig. 3. Pressure–composition diagram of CO_2 in [$C_n$mim][Tf_2N].

explained this phenomenon based on entropic rather enthalpic considerations, due to the decrease of the compounds densities with the increase of the alkyl chain length leading to a greater free volume.

The results of the application of the thermodynamic consistency test to the binary systems containing ionic liquid is presented in Table 5. In this table, NP is the number of data points, T is the temperature, k_{12}, A_{12} and A_{21} are the interaction parameters of the model, where 1 stands for the CO_2 and 2 for the ionic liquid. This table is divided in sections for each system studied. The consistency analyses for the CO_2 + [C_2mim][Tf_2N] system measured by Schilderman et al. [25] at 363.15 K are also reported here.

Some detailed results are shown in Tables 6–8. These tables are divided in two parts, the upper part shows the original data set, while the lower part shows the remaining data after removing some experimental points that have been found to be thermodynamically inconsistent. Table 6 also includes the detailed results for the system CO_2 + [C_2mim][Tf_2N] at 363.15 K by Schilderman et al. [25]. These data have deviations within the established limit values of ΔA_i, being thermodynamically consistent. In Table 7, where

Table 5
Results of the consistency test.

Reference	NP	T/K	k_{12}	A_{12}/kJ kmol^{-1}	A_{21}/kJ kmol^{-1}	$\|\Delta p\|$/%	Result
CO_2 + [C_2mim][Tf_2N]							
[17]	8	363.15	−0.1904	3767.474	−1202.621	0.7	TC
	4	293.15	−0.222	49988.291	−1791.751	0.5	TC
	9	298.15	0.0057	20355.366	−2001.440	2.4	NFC/TC
	9	303.15	−0.0090	8795.384	−1923.852	2.0	NFC/TC
	9	313.15	0.0204	5854.406	−1747.716	1.1	NFC/TC
[This work]	9	323.15	0.0108	4879.271	−1604.227	1.0	NFC/TC
	9	333.15	0.0038	4323.089	−1491.756	1.4	NFC/TC
	9	343.15	−0.0077	3830.967	−1359.963	1.6	NFC/TC
	8	353.15	−0.1468	3458.742	−1158.891	0.5	TC
	8	363.15	−0.1317	3048.107	−1016.976	0.8	TC
CO_2 + [C_5mim][Tf_2N]							
	9	298.15	0.0639	2642.548	−854.215	1.6	NFC/TC
	9	303.15	0.0606	2477.849	−773.810	1.5	NFC/TC
	9	313.15	0.0489	2232.933	−637.261	1.9	NFC/TC
[This work]	9	323.15	0.0364	2057.406	−528.352	2.4	NFC/TC
	9	333.15	0.0247	1907.507	−429.010	2.8	NFC/TC
	9	343.15	0.0195	1805.985	−356.494	2.9	NFC/TC
	9	353.15	0.0172	1728.749	−298.579	3.0	TI

Table 6
Detailed results for CO_2 (1) + [C_2mim][Tf_2N] (2) at 298.15 K.

A_P	A_ϕ	$\%\Delta A_i$	p^{exp}	p^{cal}	$\%\Delta p$	$y_1{}^{cal}$	$y_2{}^{cal}$	x_1
(8 data points) k_{12} = −0.1904, A_{12} = 3767.474, A_{21} = −1202.621, $\|\Delta p\|$(%) = 0.7								
10865327.5	10387930.5	−4.4	1.303	1.317	1.1	1.0000	0.0000	0.1230
5441391.3	5567544.7	2.3	2.543	2.514	−1.1	1.0000	0.0000	0.2120
2379790.2	2291077.1	−3.7	4.036	4.044	0.2	1.0000	0.0000	0.3030
701940.6	703925.0	0.3	6.023	5.988	−0.6	1.0000	0.0000	0.3920
78335.4	73487.2	−6.2	8.569	8.602	0.4	1.0000	0.0000	0.4790
31674.7	32701.5	3.2	10.258	10.213	−0.4	1.0000	0.0000	0.5190
4092.1	3503.8	−14.4	12.832	12.973	1.1	1.0000	0.0000	0.5700
–	–	–	14.770	14.676	−0.6	0.9999	0.0001	0.5930

detailed results at 298.15 K for the system CO_2 + [C_2mim][Tf_2N] are presented, the upper part shows that these data have deviations in the final values of ΔA_i (bold and italic type) outside the established limits; the lower part shows that when the highest area deviation is eliminated, the deviations for the remaining eight points are within the defined limits of ±20%. Therefore, although the original data set with nine data points is not fully thermodynamically consistent, the new set with the remaining eight points is thermodynamically consistent; however, the $x_{CO_2} = 0.606$ point has a good probability to be inconsistent, because two $\Delta P_i < 5$ yields $\Delta A_i > 10$.

The same procedure is applied for the data of the system CO_2 + [C_5mim][Tf_2N], at 298.15, reported in Table 8. Again, although the original data are not fully consistent, the remaining eight points, after removing one data point, are within the defined limits of −20% to +20%, which are thermodynamically consistent. Detailed results for all systems are shown in Supplementary Information. These results show that the CO_2 + [C_2mim][Tf_2N] system has greater deviations in the isopleths at x_1 = 0.75, while the CO_2 + [C_5mim][Tf_2N] system has greater deviations in the isopleths at x_1 = 0.751 and x_1 = 0.802. Therefore, the isotherms with these compositions are not fully consistent.

Table 7
Detailed results for CO_2 (1) + [C_2mim][Tf_2N] (2) at 298.15 K.

A_P	A_ϕ	$\%\Delta A_i$	p^{exp}	p^{cal}	$\%\Delta p$	$y_1{}^{cal}$	$y_2{}^{cal}$	x_1
(9 data points) k_{12} = 0.0057, A_{12} = 20355.366, A_{21} = −2001.440, $\|\Delta p\|$(%) = 2.4								
5.81E+09	5.23E+09	−9.9	0.718	0.763	6.3	1.0000	0.0000	0.221
4.34E+09	4.09E+09	−5.7	1.284	1.294	0.8	1.0000	0.0000	0.327
3.48E+09	3.30E+09	−5.2	1.915	1.889	−1.4	1.0000	0.0000	0.418
1.80E+09	1.82E+09	0.6	2.699	2.619	−3.0	1.0000	0.0000	0.503
1.09E+09	1.21E+09	10.3	3.342	3.248	−2.8	1.0000	0.0000	0.560
7.81E+08	9.40E+08	20.3	3.922	3.874	−1.2	1.0000	0.0000	0.606
7.69E+08	8.71E+08	13.4	4.540	4.618	1.7	1.0000	0.0000	0.650
3.56E+14	2.17E+15	511.2	5.520	5.759	4.3	1.0000	0.0000	0.700
–	–	–	19.065	18.939	−0.7	1.0000	0.0000	0.750
(8 data points) k_{12} = 0.2655, A_{12} = 2013.583, A_{21} = −993.493, $\|\Delta p\|$(%) = 2.4								
7.39E+09	6.72E+09	−9.2	0.718	0.754	5.0	1.0000	0.0000	0.221
6.19E+09	5.88E+09	−5.0	1.284	1.283	−0.1	1.0000	0.0000	0.327
5.45E+09	5.20E+09	−4.5	1.915	1.877	−1.9	1.0000	0.0000	0.418
2.99E+09	3.01E+09	0.9	2.699	2.609	−3.4	1.0000	0.0000	0.503
1.79E+09	1.97E+09	10.0	3.342	3.237	−3.1	1.0000	0.0000	0.560
1.16E+09	1.38E+09	18.8	3.922	3.859	−1.6	1.0000	0.0000	0.606
8.25E+08	9.02E+08	9.3	4.540	4.589	1.1	1.0000	0.0000	0.650
–	–	–	5.520	5.673	2.8	1.0000	0.0000	0.700

Table 8
Detailed results for CO_2 (1) + [C_5mim][Tf_2N] (2) at 298.15 K.

A_P	A_ϕ	$\%\Delta A_i$	p^{exp}	p^{cal}	$\%\Delta p$	$y_1{}^{cal}$	$y_2{}^{cal}$	x_1
(9 data points) k_{12} = 0.0639, A_{12} = 2642.548, A_{21} = −854.215, $\|\Delta p\|(\%)$ = 1.6								
1.11E + 12	9.85E + 11	−11.3	0.702	0.728	3.7	1.0000	0.0000	0.212
1.96E + 11	2.12E + 11	8.0	1.483	1.431	−3.5	1.0000	0.0000	0.351
2.57E + 11	2.82E + 11	9.7	1.718	1.677	−2.4	1.0000	0.0000	0.390
4.55E + 11	4.62E + 11	1.5	2.143	2.137	−0.3	1.0000	0.0000	0.453
2.23E + 10	2.14E + 10	−3.8	3.872	3.911	1.0	1.0000	0.0000	0.619
1.13E + 10	1.30E + 10	14.2	4.429	4.452	0.5	1.0000	0.0000	0.654
6.92E + 09	7.76E + 09	12.2	5.205	5.344	2.7	1.0000	0.0000	0.701
5.54E + 04	2.71E + 04	−51.0	8.065	8.036	−0.4	1.0000	0.0000	0.751
–	–	–	29.980	29.988	0.0	0.9999	0.0001	0.802
(8 data points) k_{12} = −0.1037, A_{12} = 4558.106, A_{21} = −1265.823, $\|\Delta p\|(\%)$ = 1.5								
8.94E + 11	7.86E + 11	−12.1	0.702	0.733	4.3	1.0000	0.0000	0.212
1.37E + 11	1.47E + 11	7.3	1.483	1.435	−3.2	1.0000	0.0000	0.351
1.67E + 11	1.82E + 11	8.8	1.718	1.680	−2.2	1.0000	0.0000	0.390
2.67E + 11	2.67E + 11	0.0	2.143	2.136	−0.3	1.0000	0.0000	0.453
8.66E + 09	8.21E + 09	−5.1	3.872	3.884	0.3	1.0000	0.0000	0.619
3.92E + 09	4.42E + 09	12.6	4.429	4.415	−0.3	1.0000	0.0000	0.654
2.03E + 09	2.37E + 09	16.5	5.205	5.286	1.6	1.0000	0.0000	0.701
–	–	–	8.065	8.061	−0.1	1.0000	0.0000	0.751

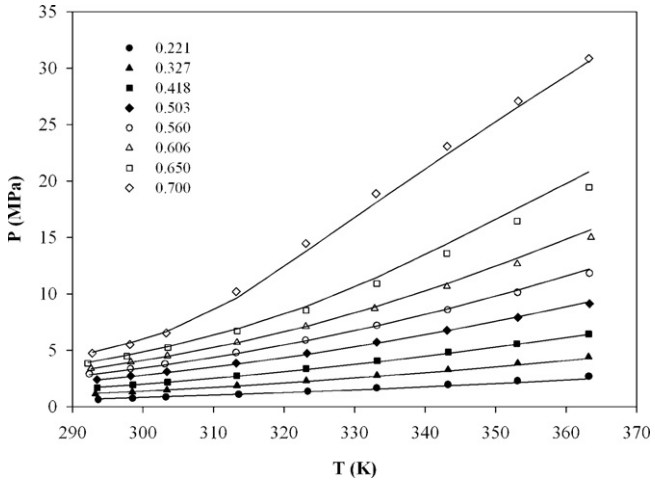

Fig. 4. PT diagram and modeling for the system CO_2 + [C_2mim][Tf_2N].

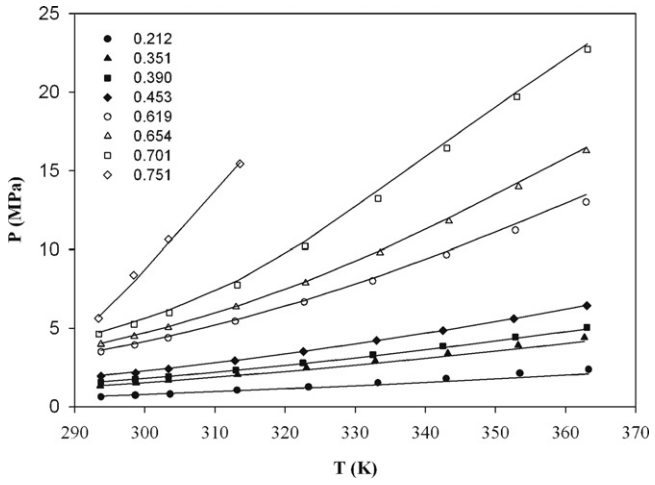

Fig. 5. PT diagram and modeling for the system CO_2 + [C_5mim][Tf_2N].

In Figs. 4 and 5 the description of the experimental data using the model detailed above and the parameters reported in Tables 1 and 9 for the CO_2 + [C_2mim][Tf_2N] and CO_2 + [C_5mim][Tf_2N] systems is presented. As can be seen, using the proposed approach it is possible to obtain a very good description of the experimental data measured in this work.

The Henry's law relates the amount of a given gas dissolved in a given type and the amount of liquid, at a constant temperature, to the fugacity of that gas in equilibrium with that liquid and can be described as

$$H_{12}(T, P) = \lim_{x_1 \to 0} \frac{f_i^L}{x_1} \quad (8)$$

where $H_{12}(T,P)$ is the Henry's constant, x_1 is the mole fraction of gas dissolved in the liquid phase, and f_1^L is the fugacity of gas in the liquid phase. As shown, Eq. (8) is only rigorously valid in the diluted region limit. The Henry's constant for the CO_2 in the ILs investigated, were estimated by fitting the PR-WS/UNIQUAC model to the data and calculating the limiting slope as the solubility approaches zero.

The results are shown in Table 10, where, $|\Delta P|$ is average absolute deviations for pressure and H_{12} is the Henry's constant calculated. For one additional validation of the calculated Henry's constant for the CO_2 + [C_2mim][Tf_2N] binary system, Henry's constant at 298.15 K and 3.56 MPa, taken from Schilderman et al. [25], was included showing good agreement with linear tendency obtained in this work. The results indicate that Henry's constant decreases slightly (i.e., CO_2 solubility increases) as the length of the carbon chain on the imidazolium ring increases.

The results for the Henry's constant of CO_2 in [C_2mim][Tf_2N] (where the calculated value 3.56 MPa at 298.15 K was included [25]) and CO_2 in [C_5mim][Tf_2N] were correlated as a function of temper-

Table 9
Estimated independent-temperature interaction parameters for the CO_2 (1) + ILs (2) systems.

System	NP	x_1	k_{12}	A_{12}/kJ kmol^{-1}	A_{21}/kJ kmol^{-1}	$\|\Delta p\|$ (%)	Max y_2[a]
CO_2 + [C_2mim][Tf_2N]	72	0.221–0.700	0.1061	4224.889	−1556.505	2.8	5.5
CO_2 + [C_5mim][Tf_2N]	63	0.212–0.751	0.0113	2613.005	−785.272	3.0	11.8

[a] These values are expressed as $y_2 \times 10^5$.

Table 10
Interaction parameter for the model and Henry's constant of CO_2 (1) + ionic liquids (2).

T/K	$\lvert\Delta p\rvert$/%	H_{12}/MPa
CO_2 + [C_2mim][Tf_2N] k_{ij} = 0. 0077, A_{12} = 2284.160, A_{21} = −723.030		
313.15	0.7	4.66
323.15	0.7	5.50
333.15	0.7	6.40
343.15	0.8	7.36
353.15	0.8	8.37
363.15	0.8	9.43
CO_2 + [C_5mim][Tf_2N] k_{ij} = 0.0113, A_{12} = 2613.005, A_{21} = −785.272		
298.15	2.7	2.88
303.15	2.1	3.18
313.15	1.8	3.81
323.15	2.6	4.49
333.15	3.3	5.24
343.15	3.8	6.03

Table 11
Coefficients A, B and C obtained for CO_2 (1) + ionic liquids (2).

Ionic liquid (%)	A	B	C	$\lvert\Delta H_{12}\rvert$
[C_2mim][Tf_2N]	−153854.908	−685.377	5.298	0.1
[C_5mim][Tf_2N]	−189365.718	−488.274	4.827	0.04

ature by an empirical equation of the type:

$$\ln(H_{12}) = A\left(\frac{1}{T}\right)^{(2)} + B\left(\frac{1}{T}\right) + C \tag{9}$$

where, the coefficients A, B and C obtained are listed in Table 11, together with the Henry's constant average absolute deviations, $\lvert\Delta H_{12}\rvert$, obtained for each ionic liquid. The average deviation of 0.1% and a maximum deviation of 0.1% for [C_2mim][Tf_2N] and an average deviation of 0.04% and a maximum deviation of 0.04% for [C_5mim][Tf_2N] were obtained.

The effect of temperature on CO_2 solubility can be related to the partial molar entropy and partial molar enthalpy of solution [59] and can be calculated from an appropriate correlation of Henry's constant:

$$\Delta_{sol}H = R\left(\frac{\partial \ln(H_{12})}{\partial(1/T)}\right)_P \tag{10}$$

$$\Delta_{sol}S = -R\left(\frac{\partial \ln(H_{12})}{\partial(1/T)}\right)_P \tag{11}$$

Table 12
Thermodynamic functions of solvation for CO_2 (1) + ionic liquids (2) at several temperatures.

T/K	$\Delta_{sol}H$/J mol^{-1}	$T\Delta_{sol}S$/(J (mol^{-1}))
[C_2mim][Tf_2N]		
298.15	−14279.3	−14162.1
303.15	−14137.8	−14096.5
313.15	−13868.3	−13872.5
323.15	−13615.5	−13669.2
333.15	−13377.8	−13425.9
343.15	−13154.0	−13177.0
353.15	−12942.9	−12890.0
363.15	−12743.4	−12601.3
[C_5mim][Tf_2N]		
298.15	−14621.1	−14549.7
303.15	−14446.9	−14429.9
313.15	−14115.2	−14123.1
323.15	−13804.0	−13830.8
333.15	−13511.5	−13492.6
343.15	−13236.1	−13142.6

The partial molar enthalpy of gas dissolution gives an indication of the strength of interactions between the gas and IL, while the partial molar entropy illustrates the amount of ordering present in the gas/IL mixture. The partial molar enthalpy values obtained are similar to those reported by Brennecke's group [21,33] and the magnitude consistent with physical absorption. The results in Table 12 show that although the partial molar enthalpy is slightly higher than the product of the temperature and the partial molar entropy they are of similar magnitude indicating that the solubility of CO_2 in ILs is not entropically driven, as suggested by some authors [22,28,60], neither essentially an enthalpic phenomena, as suggested by others [18,31], but both phenomena control the solubility of CO_2 in ILs.

5. Conclusions

A high pressure cell to measure supercritical fluid + liquid phase behavior was developed and new experimental data for CO_2 solubility in 1-ethyl-1-methyl-imidazolium bis(trifluoromethylsulfonyl)imide and 3-methyl-1-pentyl-imidazolium bis(trifluoromethylsulfonyl)imide in a wide range of temperature, pressure and carbon dioxide mole fractions are reported.

A thermodynamic consistency test based on the Peng–Robinson EoS with the Wong–Sandler/UNIQUAC mixing rule was applied to the measured data showing that they are thermodynamically consistent. The model allows a good description of the experimental data and the estimation of the Henry's constant for these systems. The partial molar enthalpies and the product of the temperature and the partial molar entropies for these systems are of similar magnitude what allows to conclude that this solubility is not driven predominantly by entropic or enthalpic phenomena, as previously admitted by various authors.

Acknowledgments

The authors are thankful for financial support from Fundação para a Ciência e a Tecnologia (Project POCI/EQU/58152/2004) and Ph.D. grant (SFRH/BD/41562/2007) of Pedro J. Carvalho. The authors would like to acknowledge FAPESP (Fundação de Amparo à Pesquisa do Estado de São Paulo), process # 2006/03711-1.

Appendix A. Supplementary data

Supplementary data associated with this article can be found, in the online version, at doi:10.1016/j.supflu.2008.10.012.

References

[1] J.A. Boon, J.A. Levisky, J.L. Pflug, J.S. Wilkes, Friedel-Crafts reactions in ambient-temperature molten salts, J. Org. Chem. 51 (1986) 480–483.
[2] S.E. Fry, N.J. Pienta, Effects of molten salts on reactions. Nucleophilic aromatic substitution by halide ions in molten dodecyltributylphosphonium salts, JACS 107 (1985) 6399–6400.
[3] H. Zhao, Innovative applications of ionic liquids as green engineering liquids, Chem. Eng. Commun. 193 (2006) 1660–1677.
[4] R. Sheldon, Catalytic reactions in ionic liquids, Chem. Commun. (2001) 2399–2407.
[5] H. Wong, S. Han, A.G. Livingston, The effect of ionic liquids on product yield and catalyst stability, Chem. Eng. Sci. 61 (2006) 1338–1341.
[6] E. Bates, R. Mayton, I. Ntai, J. Davis, CO_2 capture by a task-specific ionic liquid, JACS 124 (2002) 926–927.
[7] J.L. Anthony, E.J. Maginn, J.F. Brennecke, Solution thermodynamics of imidazolium-based ionic liquids and water, J. Phys. Chem. B 105 (2001) 10942–10949.
[8] J.G. Huddleston, H.D. Willauer, R.P. Swatloski, A.E. Visser, R.D. Rogers, Room temperature ionic liquids as novel media for clean liquid–liquid extraction, Chem. Commun. 16 (1998) 1765–1766.

[9] L. Blanchard, J. Brennecke, Recovery of organic products from ionic liquids using supercritical carbon dioxide, Ind. Eng. Chem. Res. 40 (2001) 287–292.
[10] L.A. Blanchard, D. Hancu, E.J. Beckman, J.F. Brennecke, Green processing using ionic liquids and CO_2, Nature 399 (1999) 28–29.
[11] L. Blanchard, Z. Gu, J. Brennecke, High-pressure phase behavior of ionic liquid/CO_2 systems, J. Phys. Chem. B 105 (2001) 2437–2444.
[12] A. Scurto, S. Aki, J. Brennecke, CO_2 as a separation switch for ionic liquid/organic mixtures, JACS 124 (2002) 10276–10277.
[13] A.M. Scurto, S.N.V.K. Aki, J.F. Brennecke, Carbon dioxide induced separation of ionic liquids and water, Chem. Commun. (2003) 572–573.
[14] X. Yuan, S. Zhang, J. Liu, X. Lu, Solubilities of CO_2 in hydroxyl ammonium ionic liquids at elevated pressures, Fluid Phase Equilib. 257 (2007) 195–200.
[15] J. Sun, S. Zhang, W. Cheng, J. Ren, Hydroxyl-functionalized ionic liquid: a novel efficient catalyst for chemical fixation of CO_2 to cyclic carbonate, Tetrahedron Lett. 49 (2008) 3588–3591.
[16] G. Yu, S. Zhang, X. Yao, J. Zhang, K. Dong, W. Dai, R. Mori, Design of task-specific ionic liquids for capturing CO_2: a molecular orbital study, Ind. Eng. Chem. Res. 45 (2006) 2875–2880.
[17] J. Huang, A. Riisager, R.W. Berg, R. Fehrmann, Tuning ionic liquids for high gas solubility and reversible gas sorption, J. Mol. Catal. A: Chem. 279 (2008) 170–176.
[18] M. Muldoon, S. Aki, J. Anderson, J. Dixon, J. Brennecke, Improving carbon dioxide solubility in ionic liquids, J. Phys. Chem. B 111 (2007) 9001–9009.
[19] Z. Lopez-Castillo, S. Aki, M. Stadtherr, J. Brennecke, Enhanced solubility of hydrogen in CO_2-expanded liquids, Ind. Eng. Chem. Res. 47 (2008) 570–576.
[20] M. Solinas, A. Pfaltz, P. Cozzi, W. Leitner, Enantioselective hydrogenation of imines in ionic liquid/carbon dioxide media, JACS 126 (2004) 16142–16147.
[21] S.N.V.K. Aki, B.R. Mellein, E.M. Saurer, J.F. Brennecke, High-pressure phase behavior of carbon dioxide with imidazolium-based ionic liquids, J. Phys. Chem. B 108 (2004) 20355–20365.
[22] J.L. Anderson, J.K. Dixon, J.F. Brennecke, Solubility of CO_2, CH_4, C_2H_6, C_2H_4, O_2, and N_2 in 1-hexyl-3-methylpyridinium bis(trifluoromethylsulfonyl)imide: comparison to other ionic liquids, Acc. Chem. Res. 40 (11) (2007) 1208–1216.
[23] A. Shariati, C.J. Peters, High-pressure phase behavior of systems with ionic liquids. II. The binary system carbon dioxide + 1-ethyl-3-methylimidazolium hexafluorophosphate, J. Supercrit. Fluids 29 (2004) 43–48.
[24] A. Shariati, C.J. Peters, High-pressure phase behavior of systems with ionic liquids. Part III. The binary system carbon dioxide + 1-hexyl-3-methylimidazolium hexafluorophosphate, J. Supercrit. Fluids 30 (2004) 139–144.
[25] A.M. Schilderman, S. Raeissi, C.J. Peters, Solubility of carbon dioxide in the ionic liquid 1-ethyl-3-methylimidazolium bis(trifluoromethylsulfonyl)imide, Fluid Phase Equilib. 260 (2007) 19–22.
[26] A. Finotello, J. Bara, D. Camper, R. Noble, Room-temperature ionic liquids: temperature dependence of gas solubility selectivity, Ind. Eng. Chem. Res. 47 (2008) 3453–3459.
[27] E. Shin, B. Lee, J.S. Lim, High-pressure solubilities of carbon dioxide in ionic liquids: 1-alkyl-3-methylimidazolium bis(trifluoromethylsulfonyl)imide, J. Supercrit. Fluids 45 (2008) 282–292.
[28] Y. Hou, R. Baltus, Experimental measurement of the solubility and diffusivity of CO_2 in room-temperature ionic liquids using a transient thin-liquid-film method, Ind. Eng. Chem. Res. 46 (2007) 8166–8175.
[29] B. Lee, S. Outcalt, Solubilities of gases in the ionic liquid 1-n-butyl-3-methylimidazolium bis(trifluoromethylsulfonyl)imide, J. Chem. Eng. Data 51 (2006) 892–897.
[30] M. Shiflett, A. Yokozeki, Solubility of CO_2 in room temperature ionic liquid [hmim][Tf_2N], J. Phys. Chem. B 111 (2007) 2070–2074.
[31] J. Jacquemin, M.F. Costa Gomes, P. Husson, V. Majer, Solubility of carbon dioxide, ethane, methane, oxygen, nitrogen, hydrogen, argon, and carbon monoxide in 1-butyl-3-methylimidazolium tetrafluoroborate between temperatures 283 K and 343 K and at pressures close to atmospheric, J. Chem. Thermodyn. 38 (2006) 490–502.
[32] M. Kanakubo, T. Umecky, Y. Hiejima, T. Aizawa, H. Nanjo, Y. Kameda, Solution structures of 1-butyl-3-methylimidazolium hexafluorophosphate ionic liquid saturated with CO_2: experimental evidence of specific anion–CO_2 interaction, J. Phys. Chem. B 109 (2005) 13847–13850.
[33] J. Anthony, J. Anderson, E. Maginn, J. Brennecke, Anion effects on gas solubility in ionic liquids, J. Phys. Chem. B 109 (2005) 6366–6374.
[34] C. Cadena, J. Anthony, J. Shah, T. Morrow, J. Brennecke, E. Maginn, Why is CO_2 so soluble in imidazolium-based ionic liquids? JACS 126 (2004) 5300–5308.
[35] K. Gutkowski, A. Shariati, C. Peters, High-pressure phase behavior of the binary ionic liquid system 1-octyl-3-methylimidazolium tetrafluoroborate + carbon dioxide, J. Supercrit. Fluids 39 (2006) 187–191.
[36] A. Shariati, C.J. Peters, High-pressure phase equilibria of systems with ionic liquids, J. Supercrit. Fluids 34 (2005) 171–176.
[37] J. Anthony, E. Maginn, J. Brennecke, Solubilities and thermodynamic properties of gases in the ionic liquid 1-n-butyl-3-methylimidazolium hexafluorophosphate, J. Phys. Chem. B 106 (2002) 7315–7320.
[38] V.H. Álvarez, M. Aznar, Thermodynamic modeling of vapor–liquid equilibrium of binary systems ionic liquid + supercritical {CO_2 or CHF_3} and ionic liquid + hydrocarbons using Peng–Robinson equation of state, J. Chin. Inst. Chem. Eng. 39 (2008) 353–360.
[39] José O. Valderrama, V.H. Àlvarez, A versatile thermodynamic consistency test for incomplete phase equilibrium data of high-pressure gas-liquid mixtures, Fluid Phase Equilib. 226 (2004) 149–159.
[40] D. Peng, D.B. Robinson, A new two-constant equation of state, Ind. Eng. Chem. Fundam. 15 (1976) 59–64.
[41] D.S.H. Wong, S.I. Sandler, A theoretically correct mixing rule for cubic equations of state, AIChE J. 38 (1992) 671–680.
[42] D.S. Abrams, J.M. Prausnitz, Statistical thermodynamics of liquid mixtures: a new expression for the excess Gibbs energy of partly or completely miscible systems, AIChE J. 21 (1975) 116–128.
[43] V. Álvarez, M. Aznar, Application of a thermodynamic consistency test to binary mixtures containing an ionic liquid, Open Thermodyn. J. 2 (2008) 25–38.
[44] M.G. Freire, P.J. Carvalho, A.M. Fernandes, I.M. Marrucho, A.J. Queimada, J.A. Coutinho, Surface tensions of imidazolium based ionic liquids: anion, cation, temperature and water effect, J. Colloid Interface Sci. 314 (2) (2007) 621–630.
[45] K.R. Seddon, A. Stark, M. Torres, Influence of chloride, water, and organic solvents on the physical properties of ionic liquids, Pure Appl. Chem. 72 (12) (2000) 2275–2287.
[46] J.G. Huddleston, A.E. Visser, W.M. Reichert, H.D. Willauer, G.A. Broker, R.D. Rogers, Characterization and comparison of hydrophilic and hydrophobic room temperature ionic liquids incorporating the imidazolium cation, Green Chem. 3 (2001) 156–164.
[47] R.L. Gardas, M.G. Freire, P.J. Carvalho, I.M. Marrucho, I.M.A. Fonseca, A.G.M. Ferreira, J.A.P. Coutinho, High pressure densities and derived thermodynamic properties of imidazolium based ionic liquids, J. Chem. Eng. Data 52 (1) (2007) 80–88.
[48] S. Vitu, J.N. Jaubert, J. Pauly, J.L. Daridon, D. Barth, Phase equilibria measurements of CO_2 + methyl cyclopentane and CO_2 + isopropyl cyclohexane binary mixtures at elevated pressures, J. Supercrit. Fluids 44 (2008) 155–163.
[49] J. Pauly, J. Coutinho, J.L. Daridon, High pressure phase equilibria in methane + waxy systems. 1. methane + heptadecane, Fluid Phase Equilib. 255 (2007) 193–199.
[50] S.P.M. Ventura, J. Pauly, J.L. Daridon, J.A.L. da Silva, I.M. Marrucho, A.M.A. Dias, J.A.P. Coutinho, High pressure solubility data of carbon dioxide in tri-isobutyl(methyl)phosphonium tosylate—water systems, J. Chem. Thermodyn. 40 (2008) 1187–1192.
[51] A.M.A. Dias, H. Carrier, J.L. Daridon, J.C. Pamies, L.F. Vega, J.A.P. Coutinho, I.M. Marrucho, Vapor-liquid equilibrium of carbon dioxide-perfluoroalkane mixtures: experimental data and SAFT modeling, Ind. Eng. Chem. Res. 45 (2006) 2341–2350.
[52] S.P.M. Ventura, J. Pauly, J.L. Daridon, I.M. Marrucho, A.M.A. Dias, J.A.P. Coutinho, High-pressure solubility data of methane in aniline and aqueous aniline systems, J. Chem. Eng. Data 52 (2007) 1100–1102.
[53] V.H. Álvarez, R. Larico, Y. Ianos, M. Aznar, Parameter Estimation for VLE Calculation by Global Minimization: Genetic Algorithm, Braz. J. Chem. Eng. 25 (2008) 409–418.
[54] M.G. Freire, C.M.S.S. Neves, P.J. Carvalho, R.L. Gardas, A.M. Fernandes, I.M. Marrucho, L.M.N.B.F. Santos, J.A.P. Coutinho, Mutual solubilities of water and hydrophobic ionic liquids, J. Phys. Chem. B 111 (45) (2007) 13082–13089.
[55] M.G. Freire, P.J. Carvalho, R.L. Gardas, I.M. Marrucho, L.M.N.B.F. Santos, J.A.P. Coutinho, Mutual solubilities of water and the [Cnmim][Tf2N] hydrophobic ionic liquids, J. Phys. Chem. B 112 (2008) 1604–1610.
[56] R.L. Gardas, M.G. Freire, P.J. Carvalho, I.M. Marrucho, I.M.A. Fonseca, A.G.M. Ferreira, J.A.P. Coutinho, P, (rho), T measurements of imidazolium based ionic liquids, J. Chem. Eng. Data 52 (2007) 1881–1888.
[57] P.J. Carvalho, M.G. Freire, I.M. Marrucho, A.J. Queimada, J.A.P. Coutinho, Surface tensions for the 1-alkyl-3-methylimidazolium bis(trifluoromethylsulfonyl)imide ionic liquids, J. Chem. Eng. Data 53 (2008) 1346–1350.
[58] S.G. Kazarian, B.J. Briscoe, T. Welton, Combining ionic liquids and supercritical fluids: in situ ATR–IR study of CO_2 dissolved in two ionic liquids at high pressures, Chem. Commun. (2000) 2047–2048.
[59] J.H. Hildebrand, R.L. Scott, Regular and Related Solutions, Van Nostrand Reinhold, New York, 1970.
[60] J. Anderson, J. Dixon, E. Maginn, J. Brennecke, Measurement of SO_2 solubility in ionic liquids, J. Phys. Chem. B 110 (2006) 15059–15062.
[61] Diadem Public 1.2, The DIPPR Information and Data Evaluation Manager, 2000.
[62] J. Valderrama, P. Robles, Critical properties, normal boiling temperatures, and acentric factors of fifty ionic liquids, Ind. Eng. Chem. Res. 46 (2007) 1338–1344.